Unravelling key factors controlling vivianite formation during anaerobic digestion of waste activated sludge

Hao, Xiaodi; Yu, Wenbo; Yuan, Tugui; Wu, Yuanyuan; van Loosdrecht, Mark C.M.

DOI
10.1016/j.watres.2022.118976

Publication date
2022

Document Version
Final published version

Published in
Water Research

Water Research 223 (2022) 118976

Contents lists available at ScienceDirect

Water Research

journal homepage: www.elsevier.com/locate/watres

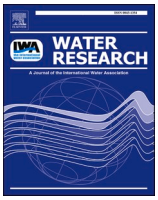

Unravelling key factors controlling vivianite formation during anaerobic digestion of waste activated sludge

Xiaodi Hao [a,*], Wenbo Yu [a], Tugui Yuan [a], Yuanyuan Wu [a], Mark C.M. van Loosdrecht [a,b]

[a] Sino-Dutch R&D Centre for Future Wastewater Treatment Technologies/Key Laboratory of Urban Stormwater System and Water Environment, Beijing University of Civil Engineering & Architecture, Beijing, 100044, China
[b] Dept. of Biotechnology, Delft University of Technology, van der Maasweg 9, 2629 HZ Delft, the Netherlands

ARTICLE INFO

Keywords:
Vivianite
Anaerobic digestion
waste activated sludge (WAS)
dissimilatory metal-reducing bacteria (DMRB)
methane-producing bacteria (MPB)
affinity constant (K_s)

ABSTRACT

As a product of phosphorous recovery from anaerobic digestion (AD) of waste activated sludge (WAS), vivianite has received increasing attention. However, key factors controlling vivianite formation have not yet been fully addressed. Thus, this study was initiated to ascertain key factors controlling vivianite formation. A simulation of chemical equilibriums indicates that interfering ions such as metallic ions and inorganic compounds may affect vivianite formation, especially at a PO_4^{3-} concentration lower than 3 mM. The experiments demonstrated that the rate of ferric bio-reduction conducted by dissimilatory metal-reducing bacteria (DMRB) and the competition of methane-producing bacteria (MPB) with DMRB for VFAs (acetate) were not the key factors controlling vivianite formation, and that ferric bio-reduction of DMRB can proceed when a sufficient amount of Fe^{3+} exists in WAS. The determined affinity constants (K_s) of both DMRB and MPB on acetate revealed that the K_{HAc} constant (4.2 mmol/g VSS) of DMRB was almost 4 times lower than that of MPB (15.67 mmol/g VSS) and thus MPB could not seriously compete for VFAs (acetate) with DMRB. As a result, vivianite formation was controlled mainly by the amount of Fe^{3+} in WAS. In practice, a Fe/P molar ratio of 2:1 should be enough for vivianite formation in AD of WAS. Otherwise, exogenously dosing Fe^{3+} or Fe^{2+} into AD must be applied in AD.

1. Introduction

Phosphorus (P), a limited and non-renewable resource for the food system and human health (van Dijk et al., 2016) is likely to be exhausted soon, in perhaps 100 years (Hao et al., 2013; Cao et al., 2019; Wu et al., 2019). As a result, a P-crisis century has started, so that P-recovery from animal wastes and wastewater is now an issue of considerable importance (Hao et al., 2013). Among others, waste activated sludge (WAS) produced in wastewater treatment plants (WWTPs) contains a considerable amount (up to 90%) of influent P-load and thus is potentially a valuable source for P-recovery (Egle et al., 2016). With this approach, the global P-recovery from WAS could meet 15–20% of the world P-demand (Li and Li, 2017; Zhang et al., 2020).

Vivianite ($Fe_3(PO_4)_2{\cdot}8H_2O$) is a remarkably stable ferrophosphorus compound (Tessadri et al., 2000), and common in anaerobic environments rich in iron and phosphorous, such as soils and deep lake sediments (Árpád et al., 2021; Rothe et al., 2016; Wu et al., 2019). Vivianite has also been found in pipelines (Prot et al., 2021) and WAS in WWTPs (Wilfert et al., 2016; Wu et al., 2019) and accounts for a majority of phosphorous and iron in anaerobic digestion (AD) of WAS (Wilfert et al., 2018). If vivianite can be recovered from WAS, a novel approach to P-recovery from wastewater may be established beyond struvite (Hao et al., 2013). Interestingly, this approach has recently attracted substantial attention, with a number of studies on it being carried out (Wilfert et al., 2016, 2018; Wang et al., 2020; Wu et al., 2020a; Zhang et al., 2020).

Fe in WAS mainly comes from ferric salt added in wastewater treatment for chemical-P removal (CPR), improving WAS dewatering performance (Wilfert et al., 2015) and preventing pipeline corrosion and H_2S generation (Wei et al., 2017). During AD of WAS, Fe^{3+} is biologically reduced to Fe^{2+} by dissimilatory metal-reducing bacteria (DMRB). At the same time, PO_4^{3-} is released from cell lysis and organic-P degradation by microorganisms in AD. As a result, vivianite can be chemically formed if the solubility product reaches its threshold ($Ksp=10^{-36}$) (Wang et al., 2020), as expressed by Eq. (1). However, other ions in AD can also combine with PO_4^{3-} or Fe^{2+} and form insoluble sediments, thus affecting vivianite formation. Metal cations, such as Ca^{2+}, Mg^{2+} and Al^{3+}, could be combined with PO_4^{3-} to form other insoluble phosphates.

* Corresponding author.
E-mail address: xdhao@hotmail.com (X. Hao).

https://doi.org/10.1016/j.watres.2022.118976
Received 27 April 2022; Received in revised form 11 July 2022; Accepted 12 August 2022
Available online 13 August 2022

Moreover, some anions, such as S^{2-}, could be combined with Fe^{2+} and thus other iron-compounds could be formed. Common interfering ions and possible reactions associated with PO_4^{3-} and Fe^{2+} are shown in Fig. S1. Some researchers have observed calcium and magnesium phosphates (Wilfert et al., 2018) and other iron-compound impurities in vivianite (Roussel and Carliell-Marquet, 2016). If vivianite can be separated and recovered from digested sludge, it would be a notable benefit, as it is not only as a P-rich compound (equivalent to struvite in the P-content) but also a high value-added product in making lithium batteries (Priambodo et al., 2017) and even as a *gem* collection (Zhang et al., 2020).

$$3Fe^{2+} + 2PO_4^{3-} + 8H_2O \rightarrow Fe_3(PO_4)_2 \cdot 8H_2O \quad (1)$$

There are two problems with vivianite recovery from AD: i) how to improve P-recovery efficiency; ii) how to separate vivianite from digested sludge. Firstly, in order to improve P-recovery efficiency it is necessary to fully understand the mechanisms of vivianite formation and to determine key controlling factors. That was the goal of this study. There are many concerns about controlling factors, such as competition of MPB and DMRB for acetate, ferric bio-reduction rate of DMRB, Fe/P ratio, interfering ions, etc. Of course, temperature and iron sources in AD would also affect vivianite formation, something that had already been demonstrated in a previous study (Cheng et al., 2017). Thus, it is essential to distinguish key factors from all other concerns. Secondly, the separation of vivianite from digested sludge is also an open topic because of tiny particles (20–100 μm) of vivianite in digested sludge (Wilfert et al., 2018), although induced crystallization by adding crystal nucleus (Liu et al., 2018) and magnetic separation had been applied for separation (Wijdeveld et al., 2022).

With this study, the effect of interfering ions on vivianite formation was first simulated with chemical software. Next, the ferric iron bio-reduction by DMRB and the competition of MPB with DMRB for VFAs were experimentally ascertained. Based on this simulation and these experiments, key factors controlling vivianite formation would be revealed.

2. Materials and methods

2.1. WAS and inoculum sludge

WAS used in this study was obtained from a sequencing batch reactor (SBR) with a working volume of 60 L. SBR was fed with synthetic wastewater (Li et al., 2019), and operated in a cycle of 22-h aeration and 2-h settlement with HRT=2 d and SRT=12 d. WAS was concentrated by the 15-μm sieve and then stored at 4 °C for use.

The inoculum sludge was cultured in a fermenter (Sartorius BIOSTAT-B plus, German), with a working volume of 4 L, operating for over 3 years. The fermenter was fed with WAS, with FeOOH simultaneously being added to the fermenter. The preparation method of FeOOH is attached in Supplementary Materials (Appendix I). The characteristics of WAS and the inoculum sludge are listed in Table 1.

Table. 1
Characteristics of the WAS and the inoculum sludge.

Parameter	WAS	Inoculum
pH	7.3 ± 0.1	6.8 ± 0.1
TS (g/L)	54.07 ± 0.13	23.5 ± 0.03
VS (g/L)	41.41 ± 0.09	13.70 ± 0.03
MLSS (g/L)	41.98 ± 0.15	17.63 ± 0.12
MLVSS(g/L)	33.88 ± 0.07	10.67 ± 0.05
VS/TS(MLSS/MLVSS)	0.766(0.807)	0.583(0.605)
P(g/L)	1.046 ± 0.033	1.172 ± 0.026
Ca(g/L)	0.921± 0.051	2.677 ± 0.137
Mg(g/L)	0.381 ± 0.009	0.126 ± 0.004
Fe(g/L)	0.097 ± 0.007	0.104 ± 0.007
Al(g/L)	0.025 ± 0.0008	0.020 ± 0.0009

2.2. Experimental set-up

2.2.1. Simulating the effects of interfering ions

Some interfering ions can affect vivianite formation, competing for PO_4^{3-} with Fe^{2+} to form other metallic P-compounds and/or affect vivianite formation The influential scenario of interfering ions can be simulated with the help of software that describes models of water chemical equilibrium (Visual MINTEQ, Version 3.1). This study focused on common cations involved in WAS, such as Ca^{2+}, Mg^{2+}, Zn^{2+} and NH+ 4 which can be combined with PO_4^{3-}, and also on common anions like S^{2-} and CO_3^{2-} which can be combined with Fe^{2+}. The P-recovery efficiency in the form of vivianite was set at 90%. The parameters approaching actual conditions applied in the simulation are attached in Supplementary Materials (Tab. S1).

2.2.2. Exploring the effect of the rate of ferric bio-reduction

Theoretically, a Fe/P molar ratio of 1.5:1 is required for vivianite formation (Eq. (1)). However, interfering ions may affect vivianite formation by consuming PO_4^{3-} and/or Fe^{2+}. Thus, a high Fe/P molar ratio was preferred for vivianite formation. In other words, enhancing the rate of ferric bio-reduction by increasing Fe^{2+} can be expected to weaken the effects of interfering ions. Because of this, it was considered that ferric bio-reduction might be one of the factors controlling vivianite formation. Therefore, a released PO_4^{3-} rate should be matched with a sufficiently high rate of ferric bio-reduction. In the experiments, however, achieving different rates of ferric bio-reduction by regulating the activity of DMRB proved challenging. Instead, directly dosing different Fe^{2+} amounts into reactors was applied to stand for different rates of ferric bio-reduction. As listed in Table 2, five tested reactors (R_1-R_5) were added with $FeCl_2$ at different testing phases, up to the same total amount of Fe^{2+}. In addition, there was a blank test (R_0) without any Fe source added, and a control test ($R_{Fe_{3+}}$) with FeOOH added (Fe^{3+} to be biologically reduced) (Zachara et al., 2002).

Based on a triplicate mode, a series of 600-mL serum bottles with a 400-mL working volume were used as batch reactors. The ratio of WAS over the inoculum sludge added in the reactors was set at 3:1 (g VSS/g VSS), based on a previous study (Hao et al., 2017). The total added iron amounts were based on the Fe/P molar ratio of 2:1.

All the reactors were adjusted pH to 7.0 ± 0.1 with NaOH (1 M) and/or HCl (1 M), then purged with nitrogen gas (N_2) for 15 min in order to remove oxygen, and finally incubated in a shaker under 35 °C. Fe^{2+} ($FeCl_2$) was added to each reactor evenly every other 12 h, as shown in Table 2.

2.2.3. Exploring the effect of mpb

As stated in the introduction, MPB inhibits vivianite formation as MPB can compete for VFAs with DMRB, especially for acetate. To suppress the activity of MPB, 2-bromoethanesulfonic acid and sodium salt ($C_2H_4BrNaO_3S$, BESA) were added to the reactors (R_6-R_{10}) with different dosages (0, 5, 20, 35 and 50 mM) along with the Fe/P molar ratio of 2:1 (FeOOH added), forming five reactors labelled from R_6 to R_{10}. Also, a blank test ($R_{0\text{-BESA}}$) was included, with 50 mM BESA added but with no FeOOH added.

Table. 2
Schedule for exploring the effect of the rate of ferric bio-reduction.

Test	Iron source	Added time*
R_0	–	–
R_{Fe3+}	FeOOH	Day 0 (once added)
R_1	$FeCl_2$	Day 0 (once added)
R_2		Day 2
R_3		Day 4
R_4		Day 7
R_5		Day 10

* Day 0: $FeCl_2$ once added on Day 0; Day 2: $FeCl_2$ evenly added during 2 d based on an interval for 12 h; and so on.

2.2.4. Determining affinity constants associated with mpb and dmrb

The activity of MPB should fit the Monod equation with single-substrate describing the relationship between reaction rate and substrate concentration, as expressed by Eq. (2). Moreover, the activity of DMRB should fit the Monod equation with double-substrate, as expressed by Eq. (3).

$$V = V_{max} \cdot \frac{S_{HAc}}{K_{HAc} + S_{HAc}} \quad (2)$$

$$V = V_{max} \cdot \frac{S_{HAc} \cdot S_{Fe}}{K_{HAc} \cdot S_{Fe} + K_{Fe} \cdot S_{HAc} + S_{HAc} \cdot S_{Fe}} \quad (3)$$

Where, V: reaction rate, mM/g VSS·d, CH_4 production rate or ferric bio-reduction rate; V_{max}: the maximum V; S_{HAc} and S_{Fe}: concentration of acetate (HAc) and Fe^{3+}, mM/g VSS; K_{HAc} and K_{Fe}: affinity constants for acetate and Fe^{3+}, mM/g VSS.

Based on the batch-test results, the affinity constants of both MPB and DMRB on acetate can be determined by fitting Eqs. (2) and (3).

2.3. Sampling and analysis

Some essential sampling and routine analysis were associated with the experiments, including:

1) mixed liquor samples were regularly collected from the reactors, and were then centrifuged and filtered via 0.45-μm membrane filters to obtain supernatants for analyzing: i) soluble PO_4^{3-} and Fe^{2+} by molybdenum blue method and phenanthroline colorimetric method using a UV spectrophotometer (Cary 5000, German Agilent Technologies company), respectively (APHA, 2005); ii) volatile fatty acids (VFAs) using Ion Chromatographer (883 Basic IC plus, Metrohm AG).
2) 1-mL sample of mixed liquor was mixed with 9 mL of HCl (1 mM) to acidize and dissolve all solid Fe^{2+} in biomass into soluble Fe^{2+} for analyzing the total Fe^{2+} concentration in mixed liquor (biomass+supernatant) (APHA, 2005).
3) Biogas production in volume was measured by a gas-liquid device and its composition was analyzed by a Gas Chromatographer (GC126, Shanghai-INSEA).
4) Other metals in mixed liquor (biomass+supernatant) were measured by inductively coupled plasma optical emission spectrometry (ICP-OES/Thermo Fisher Scientific ICAP7200/Germany) after the samples had been digested by concentrated HNO_3 and H_2O_2 under 150 °C for 2 h (Hao et al., 2017).
5) When the AD tests ended after 20 d, the samples of mixed liquor were dried out in a dark anaerobic oven at 45 °C to prevent vivianite from being oxidized. Then, the dried samples were ground to powders (<0.2 mm) to confirm the existence of vivianite by using X-ray diffraction (XRD), as shown in Fig. S2, and also to determine the amount of vivianite formation by the method of chemical sequential extraction according to a previous study (Uhlmann et al., 1990), which is attached in Supplementary Materials (Tab. S2). The extraction can be divided into 5 forms of P-compounds: Labile-P, MCO_3-P, Fe-P, Ca-P, and Residual-P; among them, Fe-P includes Fe-bound P, Al-bound P as well as organic-P. As both WAS and the inoculum sludge contained little Al (Table 1) and also only small amounts of organic-P, Fe-P in the dried samples could be regarded as vivianite, at least approximatively (Wang et al., 2021; Wilfert et al., 2016).
6) The microbial community of mixed liquor was detected using the high-throughput sequencing method. The genomic DNA was extracted and amplified by PCR with 515FmodF (5′-GTGYCA GCMGCCGCGGTAA-3′) and 806RmodR (5′-GGACTA CNVGGGTWTCTAAT-3′) primer pair.

3. Results and discussion

3.1. Effects of interfering ions

The simulation demonstrates that the presence of interfering ions can seriously affect vivianite formation, especially at a lower PO_4^{3-} concentration (<3 mM), as shown in Fig. 1. Clearly, the required amount of Fe^{2+} for vivianite formation increases significantly in the presence of interfering ions; the Fe/P molar ratio increases from 1.5 to 5.5 at PO_4^{3-} = 1 mM to obtain the same amount of vivianite. Above PO_4^{3-} = 5 mM/L, vivianite formation would not be greatly affected by the Fe/P molar ratio. Based on Eq. (1), a sufficient amount of Fe^{2+} is one of the factors controlling vivianite formation, with interfering ions making the required Fe^{2+} amount considerably higher. As a result, the rate of ferric bio-reduction is crucial in vivianite formation during AD.

According to a previous study (Shiba and Ntuli, 2017), the total P-concentration in WAS is generally between 6.76 and 25.69 mM/L, and the measured P-concentration in the reactors was around 11.7 mM/L. The simulation reveals that the lowest required Fe/P ratio is 1.94 and thus the Fe/P ratio was set at 2 to meet the needs of vivianite formation.

3.2. Effects of the rate of ferric bio-reduction

Fig. 2 presents the effect of the rate of ferric bio-reduction on vivianite formation. Fig. 2a indicates the results of sequential phosphorus extraction fraction in sludge from the reactors. The Fe-P percentage in the blank test (R_0) was the lowest one in all the reactors due to no exogenous Fe being added. All the reactors in which $FeCl_2$ was added (R_1-R_5) tended to have almost the same on the Fe-P percentage, 80.2–87.5%. The reactor with FeOOH added (R_{Fe3+}) had a 65% Fe-P percentage although it had the same amount of Fe^{3+} as Fe^{2+} added ($FeCl_2$) in R_1-R_5. An almost identical Fe-P percentage in R_1-R_5 revealed that vivianite may be formed for a trial period of 20 d no matter what the "rate ferric bio-reduction" is. Relatively, the same Fe^{3+} amount in R_{Fe3+} as Fe^{2+} in R_1-R_5 did not produce the same amount of vivianite formation.

The above phenomena could be explained by the process of ferric bio-reduction. When Fe^{3+} in the form of FeOOH was biologically reduced into Fe^{2+}, a part of Fe^{2+} was instantly combined with Fe^{3+} in FeOOH and formed Fe_3O_4 (Zachara et al., 2002). Then, Fe_3O_4 gradually reacted with PO_4^{3-} in solution and formed vivianite (O'Loughlin et al., 2013). Thus, the speed of vivianite formation by ferric bio-reduction was slower than that of directly dosing $FeCl_2$. Moreover, $FeCl_2$ could be completely dissolved in solution when added. In this way, Fe^{2+} could also replace and exchange other metal ions already combined with PO_4^{3-} for vivianite formation besides its direct combination with PO_4^{3-}. As a result, R_1-R_5 had more vivianite formation than R_{Fe3+}.

According to the total Fe^{2+} concentration (biomass+supernatant) which was measured from mixed liquor (all acidized into Fe^{2+} by HCl) (Fig. 2b), the rate of ferric bio-reduction conducted by DMRB in R_{Fe3+} increased quickly during the first three days, and then became a Fe^{2+}-plateau between 4 and 7 d, finally followed by another fast increase. The first increase in Fe^{2+} demonstrated that there was already a sufficient amount of VFAs at the beginning of ferric bio-reduction. Then, VFAs became exhausted by both DMRB and MPB and thus ferric bio-reduction reaction was inhibited by VFAs. In about 3 d, accumulation of VFAs by acidification occurred again and then the second increase of Fe^{2+} appeared, till its maximal value was equivalent to the totally added $FeCl_2$ in R_1-R_5. Anyway, a full ferric bio-reduction was achieved within 10 d. The high-throughput sequencing data revealed that the main DMRB involved in the reaction was genus *Rhodoferax ferrireducens*, as can be seen in (Fig. 3 and Tab. S3). *R. ferrireducens* could utilize acetate as the only carbon source, which could not use other common short chain VFAs (Finneran et al., 2003; Lovley et al., 2004). Clearly, MPB also utilized acetate for CH_4 production. Therefore, MPB could compete for acetate with DMRB and limit the rate of ferric bio-reduction if acetate

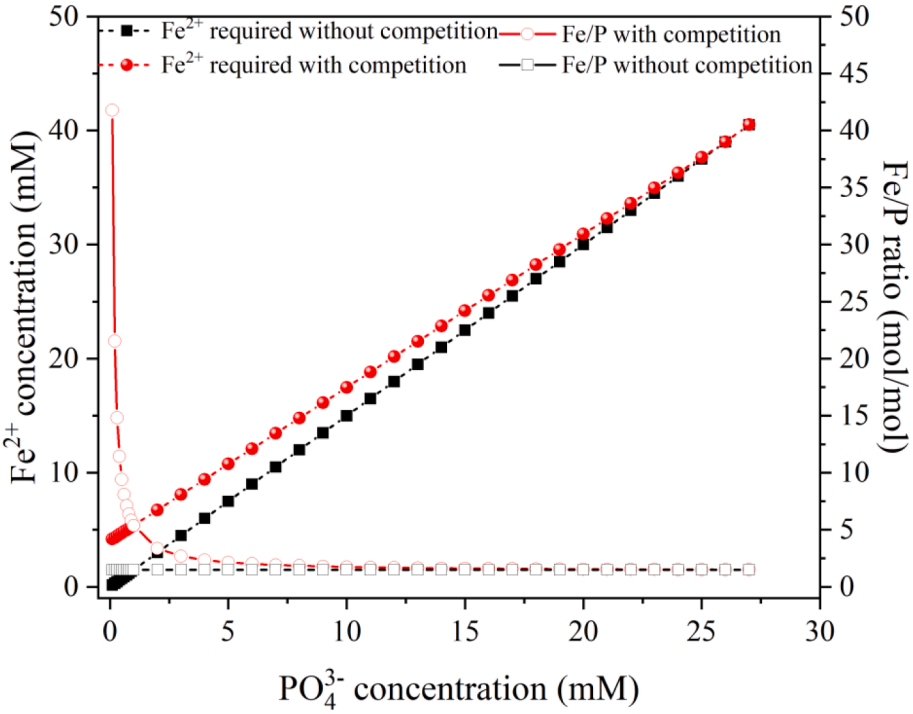

Fig. 1. Fe^{2+} amount and Fe/P molar ratio required for vivianite formation with and without interfering ions.

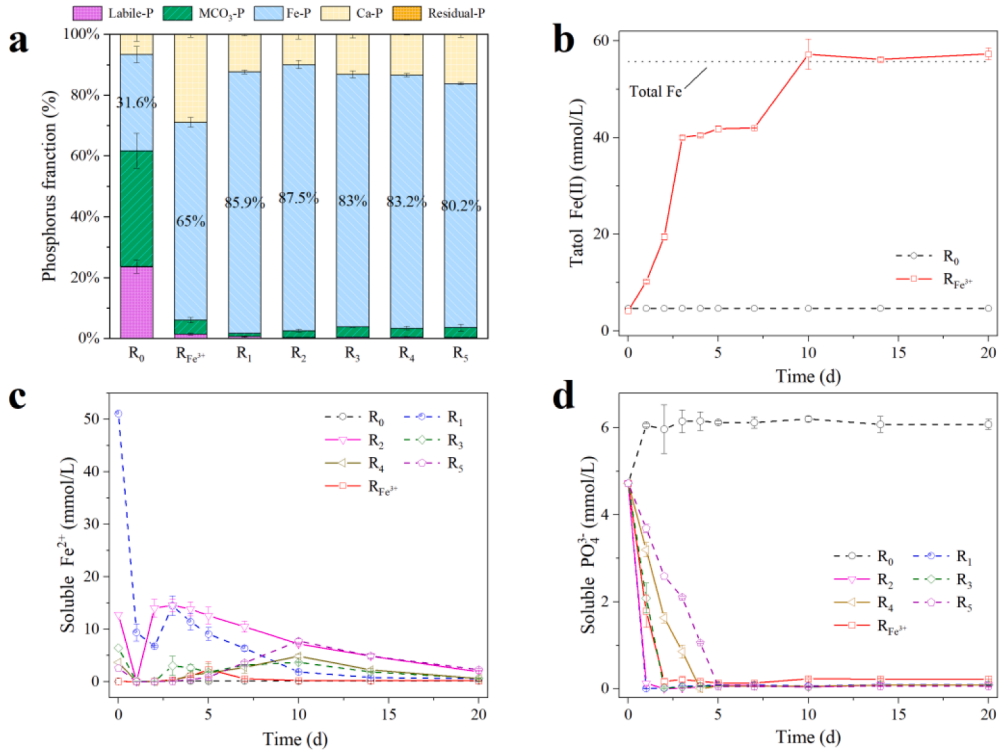

Fig. 2. Sequential phosphorus extraction fraction (a), total Fe^{2+} concentration (b), soluble Fe^{2+} (c) and soluble PO_4^{3-} (d).

was insufficient.

Combined with Figs. 2c and 2d, the rates of ferric bio-reduction and vivianite formation can be further evaluated. The dosed $FeCl_2$, as in R_1 and R_2, began with a fast decrease and then proceeded to increase, finally experiencing a gradual decrease in Fe^{2+}. The first quick decrease can be attributed to the dual function of chemical combination (to vivianite) and biological and/or chemical adsorption, and then gradually released into solution to be combined by PO_4^{3-} and other anionic compounds (Fig. 2c). Relatively, the Fe^{2+} amount in R_{Fe3+} was at a lower level due to ferric bio-reduction and continual combination into vivianite; a small peak of Fe^{2+} appeared between 4 and 7 d (Fig. 2c), which was caused by lack of acetate, corresponding to the Fe^{2+}plateau in Fig. 2b.

Fig. 2d reveals that PO_4^{3-} tended to a fast decrease in all the reactors

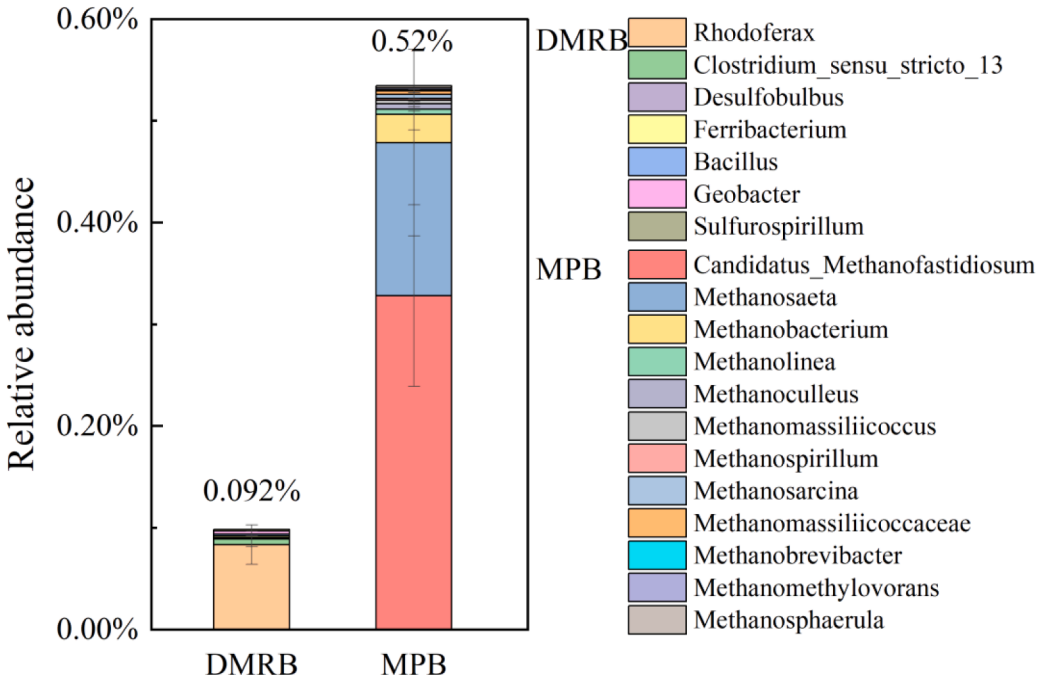

Fig. 3. Relative abundance of DMRB and MPB.

(except for the blank). Interestingly, the decrease in PO_4^{3-} in R_{Fe3+} did not lag too much behind the quickly dosing $FeCl_2$ in R_1 and R_2, accomplished within 2 d and only 1 d shorter than that in R_1 and R_2. Even for the slowly dosing $FeCl_2$ in R_4 and R_5, the decrease on PO_4^{3-} was also quick, being accomplished within 5 d.

On the SRT scale ($\geq$ 20 d) of AD, the rate of ferric bio-reduction was obviously not a key factor controlling vivianite formation. Especially based on the decreasing tendency of PO_4^{3-} (Fig. 2d), more Fe^{2+} did not combine with more PO_4^{3-} in vivianite formation. Furthermore, the residual Fe^{2+} in all of the reactors after vivianite formation (within 1–5 d) might be combined by other anionic compounds rather than PO_4^{3-} (Fig. 2c).

3.3. Associated microbial community

The relative abundance of DMRB and MPB determined by high-throughput sequencing is shown in Fig. 3, and some parameters about *R. ferrireducens* are shown as Tab. S3. As shown in Fig. 3, *R. ferrireducens* was determined as a major species of DMRB, accounting for more than 90% of DMRB and for 0.08%−0.12% of the total biomass population, figures that are consistent with a previous study (Wang et al., 2019). The reason could be attributed to: i) competitive survival strategy in a low-acetate and high-ammonia environment with greater energy efficiency (Zhuang et al., 2011); ii) varied energy conversion pathways, PHA synthesis for energy storage (Finneran et al., 2003) and co-occurrence with *Methanosarcina* at lack of Fe^{3+} (Yee and Rotaru, 2020); iii) resistance to multiple environmental factors such as heavy metals, aromatic compounds and nutrient limitation, etc. (Risso et al., 2009). These features enabled *R. ferrireducens* to adapt quickly to AD and to become the major species of DMRB.

Fig. 3 also reveals that MPB accounted for 0.52% of the total biomass population, which is 5.7 times higher than DMRB. Clearly, both MPB and DMRB needed to metabolize VFAs. Thus, it seemed as if there would be a competition for VFAs between them. Due to differences in physiological characteristics, DMRB and MPB adopted different survival strategies. DMRB could oxidize acetate completely and produce energy, but they were often limited by the amount of electron acceptors, i.e., Fe^{3+}. Thus, storing energy and reducing their growth rate may be a survival strategy of DMRB to avoid potential energy shortages. Conversely, MPB could convert acetate completely into CH_4 and obtain energy in time for growth. Because of this, the population of MPB was higher than that of DMRB.

3.4. Effects of methane-producing bacteria (MPB)

3.4.1. Inhibited activity of mpb

With BESA increasingly added to the reactors, the activity of MPB was gradually inhibited and the CH_4 production tended to decrease, as shown in Supplementary Materials (Fig. S3). With 50 mg/L of BESA dosed in R_{10}, CH_4 production almost totally ceased. Thus, the blank reactor ($R_{0\text{-BESA}}$) was added with 50 mg/L of BESA. Under these circumstances, the interferences of MPB on DMRB were fully eliminated.

3.4.2. Vivianite formation without the interference of mpb

Fig. 4 recorded the conditions of vivianite information when MPB was inhibited. As shown in Fig. 4a, vivianite formation gradually increased from 66.8% to 75.7% along with increased dosages of BESA, indicating that the inhibited activity of MPB could be helpful for DMRB and also for vivianite formation. Compared to the results shown in Fig. 2a (R_{Fe3+}: 65% vivianite), however, the maximal vivianite formation under the inhibited conditions of MPB was only reached 75.7% (R_{10}, with 50 mg/L of BESA added), demonstrating an increase by about 10% in vivianite formation. The compared results revealed that MPB affected DMRB on consuming VFAs (acetate) but its influential extent on DMRB was only a minor factor.

An interesting phenomenon occurred in the blank reactor ($R_{0\text{-BESA}}$), in which the amount of vivianite formation (21.7%) was about 10% less than that in R_0 (31.6%, Fig. 2a). When the activity of MPB was totally inhibited in $R_{0\text{-BESA}}$, vivianite formation should increase, in principle, even though no FeOOH was added (both blanks could utilize residual Fe^{3+} contained in WAS and the inoculum sludge). This phenomenon could be explained by two factors: decreased pH and/or increased CO_2 in $R_{0\text{-BESA}}$. First, a lower pH was not beneficial to vivianite formation although vivianite can be formed in a wide pH range (6–9) (Liu et al., 2018); the pH values in R_0 and $R_{0\text{-BESA}}$ were 7.2 and 6.8, respectively. When BESA was added in $R_{0\text{-BESA}}$, the CH_4 production was inhibited and acidification (Fig. 4b) gradually decreased pH, which was not favorable to vivianite formation.

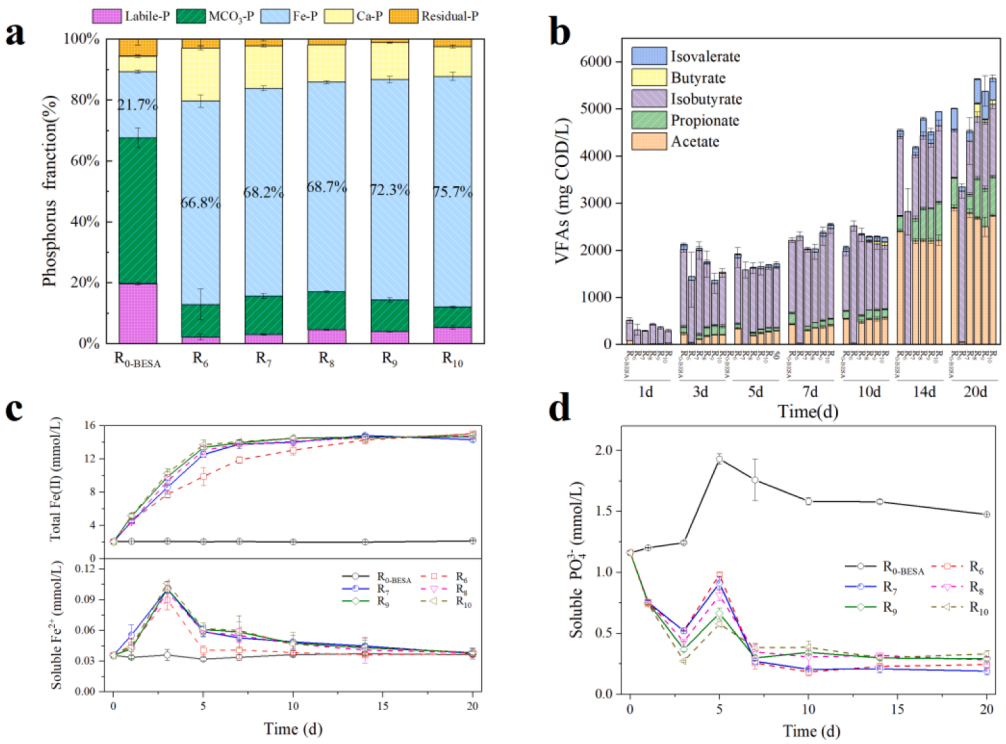

Fig. 4. Vivianite formation with MPB inhibited: phosphorus extraction fraction (a); VFAs concentration (b); total Fe^{2+} concentration (c); soluble PO_4^{3-}(d).

Second, the concentration of CO_2 in $R_{0\text{-BESA}}$ would increase due to the inhibited activity of MPB, which generally caused the increased concentration of CO2–3 due to a greater partial pressure of CO_2 in the reactor (Sander, 2015). As a result, MCO_3-P would increase and thus vivianite formation was inhibited. Based on the content of MCO_3-P in both R_0 and $R_{0\text{-BESA}}$, the latter was about 10% higher than the former, which corresponded closely to the difference of 10% in vivianite formation.

The same phenomenon also occurred in the other reactors (R_7 to R_{10}). From this aspect, vivianite formation recorded in Fig. 4a shows a comprehensive (net) result of vivianite formation enhanced by inhibiting MPB and the appearance of MCO_3-P due to CO_2 formed.

This tendency of VFAs (Fig. 4b) demonstrates that a higher dosage of BESA was needed to inhibit the activity of MPB. With 50 mg/L of BESA dosed in, the activity of MPB was almost completely inhibited, which can be seen from the accumulated VFAs at the end of the tests (20 d): more VFAs including acetate were left over. However, there were lower concentrations of VFAs in R6 without BESA dosed in and no acetate was left over at the end of the tests, indicating that MPB were consuming acetate for CH_4 production at the same time as vivianite formation.

The effects of MPB on DMRB competing for acetate can be also demonstrated by the process of ferric bio-reduction, as shown in Fig. 4c. Due to the competition of MPB, the total amount of Fe^{2+} in R_6 gradually reached its maximal value on 15 d, but the other reactors (R_7-R_{10}) completed the process of ferric bio-reduction on 5 d. However, the fast process of ferric bio-reduction in R_7-R_{10} exerted little effect on vivianite formation as the descending tendency of PO_4^{3-} was almost the same as that in R_6 (Fig. 4d), showing that vivianite formation also depended on the instantly available amount of PO_4^{3-} released from bacterial cells.

With Fig. 4c (the lower half) and Fig. 4d combined for analysis in the initial period of the tests (prior to 3 d), the rate of ferric bio-reduction in R_6-R_{10} was enough to be combined with already released PO_4^{3-} at that time, indicating that soluble Fe^{2+} increased and soluble PO_4^{3-} dropped prior to 3 d Then, soluble Fe^{2+} got down and soluble PO_4^{3-} increased, revealing that more PO_4^{3-} was released from bacterial cells (Wang et al., 2022) and the rate of ferric bio-reduction that emerged was insufficient to be combined with PO_4^{3-} released for vivianite formation, till 5 d. In 5 d, the release of PO_4^{3-} became slow and reduced Fe^{2+} could be gradually combined with all released PO_4^{3-} for vivianite formation in 2 d.

In short, the inhibited activity of MPB was somehow helpful for the ferric bio-reduction to a minor extent but more acetate available for DMRB did not stimulate vivianite formation quickly.

3.4.3. *Fitting the curves to the monod equation*

Based on the results from R_6 without BEAS added (mixed culture), the fitting curves to the Monod equation for both MPB and DMRB are illustrated in Fig. 5, and the key fitting data are shown in Table 3. The fitting method and process is attached in Supplementary Materials (Appendix II). Although there was competition between MPB and DMRB for acetate, the K_{HAc} constant (4.2 mM/g VSS) of DMRB was almost 4 times lower than that (15.67 mM/g VSS), which implied that DMRB could react at a lower acetate concentration than MPB. Clearly, this valuable finding on the affinity constants of DMRB and MPB based on acetate was a reason that MPB could not inhibit DMRB to a large extent, as analyzed above. Moreover, K_{HAc}=15.67 mM/g VSS of MPB determined in this study approaches the 13.3 mM/g VSS obtained in a previous study (Conklin et al., 2006).

3.5. *Discussion*

Based on the above analysis, interfering ions could affect vivianite formation, especially at a lower PO_4^{3-} concentration (<3 mM, as shown in Fig. 1). However, the PO_4^{3-} concentration in this study was generally above 3 mM. Thus, vivianite formation was not interfered with by PO_4^{3-}. Under these circumstances, the amount of Fe^{3+} existing in WAS became a key factor controlling vivianite information. In the tests, the Fe/P molar ratio of 2:1 was exerted and so the amount of Fe^{3+} was more than enough for ferric bio-reduction and vivianite formation to take place. In practice, however, exogenously dosing Fe^{3+} is necessary when the amount of Fe^{3+} existing in WAS is not enough, or directly dose Fe^{2+} into AD when applicable.

Fe^{3+} in AD must be biologically reduced to Fe^{2+} by DMRB to form

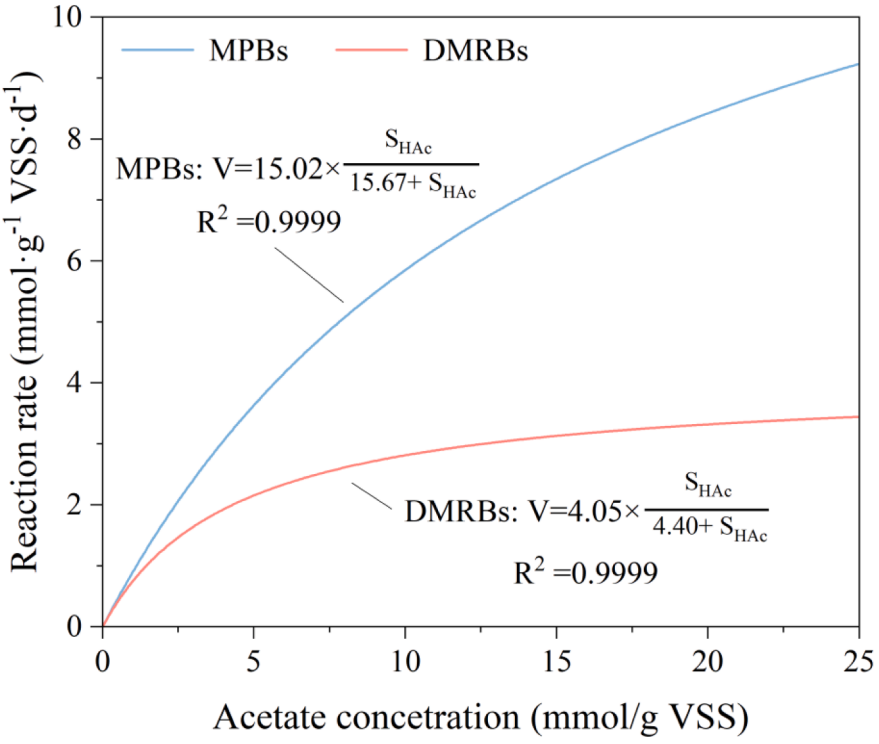

Fig. 5. Fitting curves of the Monod equation for MPB and DMRB based on acetate in R_6.

Table. 3
The fitting results of Monod equation for MPB and DMRB in R_6.

Bacteria	V_{max}/mM·d^{-1}	K_{HAc} /mM·g^{-1} VSS	K_{Fe} /mM·g^{-1} VSS
DMRB	4.05	4.40	14.27
MPB	15.02	15.67	–

vivianite. Therefore, the rate of ferric bio-reduction is an important issue. However, the results demonstrate that, while the rate of ferric bio-reduction was indeed a factor controlling vivianite formation, it was not the key factor. As long as there were sufficient amounts of Fe^{3+} in AD, vivianite formation would not be a problem and a considerable amount of vivianite could be expected.

Then, the attention for the study was turned to the competition from MPB for VFAs (acetate) with DMRB. Unexpectedly, completely inhibiting MPB activity did not contribute greatly to vivianite formation although full acetate became available for DMRB (*R. ferrireducens,* a major species only utilizing acetate as carbon source). In other words, acetate was not a key factor controlling vivianite formation, and did not inhibit the ferric bio-reduction rate to a large extent.

The determined affinity constants (K_s) of DMRB and MPB based on acetate reveal that K_{Hac} of DMRB being almost four times lower than that of MPB was a key reason for the weaker competition from MPB based on acetate with DMRB.

In conclusion, vivianite formation in AD was mainly due to there being enough Fe^{3+} contained in WAS, which not only needed to match the amount of PO_4^{3-} released from bacterial cells but also required consideration of the effect of interfering ions. In practice, a Fe/P molar ratio of 2:1 is sufficient for vivianite formation.

As DMRB could compete with MPB for acetate, the phenomenon of reduced CH_4 production would occur with vivianite recovery, which could affect energy recovery from WWTPs. Thus, balancing the recoveries of energy and vivianite is something that future research should focus on.

4. Conclusions

Based on the above analysis and discussion, some conclusions can be drawn, as follows:

- Interfering ions could affect vivianite formation, especially at a lower PO_4^{3-} concentration (<3 mM). However, the condition affected by PO_4^{3-} did not occur, as at least 10 mM of PO_4^{3-} existed in the tests.
- The rate of ferric bio-reduction was one factor controlling vivianite formation, but not the key one, as it only inhibited vivianite formation to a slight extent.
- *Rhodoferax ferrireducens* was determined as a major species of DMRB, accounting for more than 90% of DMRB and for 0.08–0.12% of the total biomass population, which was an acetate-dependent species.
- The inhibited activity of MPB was somehow helpful for ferric bio-reduction to a slight extent but more acetate available for DMRB did not stimulate vivianite formation quickly.
- The difference in the affinity constants (K_{HAc}) of DMRB and MPB based on acetate reveals that vivianite formation was not inhibited by MPB or acetate.
- Vivianite formation in AD mainly depended on sufficient amounts of Fe^{3+} existing in WAS, with an Fe/P molar ratio of 2:1 being enough for vivianite formation in AD of WAS.

Declaration of competing interest

The authors declare that they have no known competing financial interests or personal relationships that could have appeared to influence the work reported in this paper.

Data Availability

Data will be made available on request.

Acknowledgements

The study was financially supported by the National Natural Science Foundation of China (51878022) and Beijing Energy Conservation & Sustainable Urban and Rural Development Provincial and Ministry Co-construction Collaboration Innovation Center (2022). We thank Mr. Rowan Kohll for reviewing our use of English grammar and writing style.

Supplementary materials

Supplementary material associated with this article can be found, in the online version, at doi:10.1016/j.watres.2022.118976.

References

APHA, 2005. Standard Methods for the Examination of Water and Wastewater. Am. Public Heal. Assoc. Am. Water Work. Assoc.

Árpád, C., Lajos, P., Ferenc, K., Sándor, S., Péter, R., 2021. Vivianite formation as indicator of human impact in porous sediments. Environ. Earth Sci. 80 (17), 1–17. https://doi.org/10.1007/s12665-021-09866-2.

Cao, J., Wu, Y., Zhao, J., Jin, S., Aleem, M., Zhang, Q., Fang, F., Xue, Z., Luo, J., 2019. Phosphorus recovery as vivianite from waste activated sludge via optimizing iron source and pH value during anaerobic fermentation. Bioresour. Technol. 293 https://doi.org/10.1016/j.biortech.2019.122088.

Cheng, X., Wang, J., Chen, B., Wang, Y., Liu, J., Liu, L., 2017. Effectiveness of phosphate removal during anaerobic digestion of waste activated sludge by dosing iron(III). J. Environ. Manage. 193, 32–39. https://doi.org/10.1016/j.jenvman.2017.02.009.

Conklin, A., Stensel, H.D., Ferguson, J., 2006. Growth kinetics and competition between Methanosarcina and Methanosaeta in mesophilic anaerobic digestion. Water Environ. Res. 78 (5), 486–496. https://doi.org/10.2175/106143006×95393.

Egle, L., Rechberger, H., Krampe, J., Zessner, M., 2016. Phosphorus recovery from municipal wastewater: an integrated comparative technological, environmental and economic assessment of P recovery technologies. Sci. Total Environ. 571, 522–542. https://doi.org/10.1016/j.scitotenv.2016.07.019.

Finneran, K.T., Johnsen, C.v., Lovley, D.R., 2003. Rhodoferax ferrireducens sp. nov., a psychrotolerant, facultatively anaerobic bacterium that oxidizes acetate with the reduction of Fe(III). Int. J. Syst. Evol. Microbiol. 53 (3), 669–673. https://doi.org/10.1099/ijs.0.02298-0.

Hao, X., Wei, J., van Loosdrecht, M.C.M., Cao, D., 2017. Analysing the mechanisms of sludge digestion enhanced by iron. Water Res. 117, 58–67. https://doi.org/10.1016/j.watres.2017.03.048.

Hao, X., Wang, C., Van Loosdrecht, M.C.M., Hu, Y., 2013. Looking beyond struvite for P-recovery. Environ. Sci. Technol. https://doi.org/10.1021/es401140s.

Li, J., Hao, X., van Loosdrecht, M.C.M., Luo, Y., Cao, D., 2019. Effect of humic acids on batch anaerobic digestion of excess sludge. Water Res. 155, 431–443. https://doi.org/10.1016/j.watres.2018.12.009.

Li, R.h., Li, X.y., 2017. Recovery of phosphorus and volatile fatty acids from wastewater and food waste with an iron-flocculation sequencing batch reactor and acidogenic co-fermentation. Bioresour. Technol. 245, 615–624. https://doi.org/10.1016/j.biortech.2017.08.199.

Liu, J., Cheng, X., Qi, X., Li, N., Tian, J., Qiu, B., Xu, K., Qu, D., 2018. Recovery of phosphate from aqueous solutions via vivianite crystallization: thermodynamics and influence of pH. Chem. Eng. J. 349, 37–46. https://doi.org/10.1016/j.cej.2018.05.064.

Lovley, D.R., Holmes, D.E., & Nevin, K.P. (2004). Dissimilatory Fe(III) and Mn(IV) reduction. In Advances in Microbial Physiology (Vol. 49, Issue Iii). https://doi.org/10.1016/S0065-2911(04)49005-5.

O'Loughlin, E.J., Boyanov, M.I., Flynn, T.M., Gorski, C.A., Hofmann, S.M., McCormick, M.L., Scherer, M.M., Kemner, K.M., 2013. Effects of bound phosphate on the bioreduction of lepidocrocite (γ-FeOOH) and maghemite (γ-Fe2O3) and formation of secondary minerals. Environ. Sci. Technol. 47 (16), 9157–9166. https://doi.org/10.1021/es400627j.

Priambodo, R., Shih, Y.J., Huang, Y.H., 2017. Phosphorus recovery as ferrous phosphate (vivianite) from wastewater produced in manufacture of thin film transistor-liquid crystal displays (TFT-LCD) by a fluidized bed crystallizer (FBC). RSC Adv., 7 (65), 40819–40828. https://doi.org/10.1039/c7ra06308c.

Prot, T., Korving, L., Dugulan, A.I., Goubitz, K., van Loosdrecht, M.C.M., 2021. Vivianite scaling in wastewater treatment plants: occurrence, formation mechanisms and mitigation solutions. Water Res. 197, 117045 https://doi.org/10.1016/j.watres.2021.117045.

Risso, C., Sun, J., Zhuang, K., Mahadevan, R., DeBoy, R., Ismail, W., Shrivastava, S., Huot, H., Kothari, S., Daugherty, S., Bui, O., Schilling, C.H., Lovley, D.R., Methé, B. A., 2009. Genome-scale comparison and constraint-based metabolic reconstruction of the facultative anaerobic Fe(III)-reducer Rhodoferax ferrireducens. BMC Genomics 10, 447. https://doi.org/10.1186/1471-2164-10-447.

Rothe, M., Kleeberg, A., Hupfer, M., 2016. The occurrence, identification and environmental relevance of vivianite in waterlogged soils and aquatic sediments. Earth Sci. Rev. 158, 51–64. https://doi.org/10.1016/j.earscirev.2016.04.008.

Roussel, J., Carliell-Marquet, C., 2016. Significance of vivianite precipitation on the mobility of iron in anaerobically digested sludge. Front. Environ. Sci. 4 (SEP), 1–12. https://doi.org/10.3389/fenvs.2016.00060.

Sander, R., 2015. Compilation of Henry's law constants (version 4.0) for water as solvent. Atmos. Chem. Phys. 15 (8), 4399–4981. https://doi.org/10.5194/acp-15-4399-2015.

Shiba, N.C., Ntuli, F., 2017. Extraction and precipitation of phosphorus from sewage sludge. Waste Manage. (Oxford) 60, 191–200. https://doi.org/10.1016/j.wasman.2016.07.031.

Tessadri, R., 2000. Vivianite from the iceman of the Tisenjoch (Tyrol, Austria): mineralogical-chemical data. The Iceman and His natural environment, 137–141. https://doi.org/10.1007/978-3-7091-6758-8_11.

Uhlmann, D., Röske, I., Hupfer, M., Ohms, G., 1990. A simple method to distinguish between polyphosphate and other phosphate fractions of activated sludge. Water Res. 24 (11), 1355–1360. https://doi.org/10.1016/0043-1354(90)90153-W.

van Dijk, K.C., Lesschen, J.P., Oenema, O., 2016. Phosphorus flows and balances of the European Union Member States. Sci. Total Environ. 542, 1078–1093. https://doi.org/10.1016/j.scitotenv.2015.08.048.

Wang, Q., Kim, T.H., Reitzel, K., Almind-Jørgensen, N., Nielsen, U.G., 2021. Quantitative determination of vivianite in sewage sludge by a phosphate extraction protocol validated by PXRD, SEM-EDS, and 31P NMR spectroscopy towards efficient vivianite recovery. Water Res. 202 (May), 1–9. https://doi.org/10.1016/j.watres.2021.117411.

Wang, R., Wilfert, P., Dugulan, I., Goubitz, K., Korving, L., Witkamp, G.J., van Loosdrecht, M.C.M., 2019. Fe(III) reduction and vivianite formation in activated sludge. Sep. Purif. Technol 220, 126–135. https://doi.org/10.1016/j.seppur.2019.03.024.

Wang, S., Wu, Y., An, J., Liang, D., Tian, L., Zhou, L., Wang, X., Li, N., 2020. Geobacter autogenically secreted fulvic acid to facilitate the dissimilated iron reduction and vivianite recovery. Environ. Sci. Technol. https://doi.org/10.1021/acs.est.0c01404.

Wang, Y., Zheng, K., Guo, H., Tong, Y., Zhu, T., Liu, Y., 2022. Unveiling the mechanisms of how vivianite affects anaerobic digestion of waste activated sludge. Bioresour. Technol. 343, 126045 https://doi.org/10.1016/j.biortech.2021.126045. August 2021.

Wei, Y., Dai, J., Mackey, H.R., Chen, G.H., 2017. The feasibility study of autotrophic denitrification with iron sludge produced for sulfide control. Water Res. 122, 226–233. https://doi.org/10.1016/j.watres.2017.05.073.

Wijdeveld, W.K., Prot, T., Sudintas, G., Kuntke, P., Korving, L., van Loosdrecht, M.C.M., 2022. Pilot-scale magnetic recovery of vivianite from digested sewage sludge. Water Res. 212, 118131 https://doi.org/10.1016/j.watres.2022.118131. April 2021.

Wilfert, P., Dugulan, A.I., Goubitz, K., Korving, L., Witkamp, G.J., van Loosdrecht, M.C.M., 2018. Vivianite as the main phosphate mineral in digested sewage sludge and its role for phosphate recovery. Water Res. 144, 312–321. https://doi.org/10.1016/j.watres.2018.07.020.

Wilfert, P., Kumar, P.S., Korving, L., Witkamp, G.J., & van Loosdrecht, M.C.M., 2015. The relevance of phosphorus and iron chemistry to the recovery of phosphorus from wastewater: a review. In Environmental Science and Technology (Vol. 49, Issue 16). https://doi.org/10.1021/acs.est.5b00150.

Wilfert, P., Mandalidis, A., Dugulan, A.I., Goubitz, K., Korving, L., Temmink, H., Witkamp, G.J., van Loosdrecht, M.C.M., 2016. Vivianite as an important iron phosphate precipitate in sewage treatment plants. Water Res. 104, 449–460. https://doi.org/10.1016/j.watres.2016.08.032.

Wu, Y., Cao, J., Zhang, Q., Xu, R., Fang, F., Feng, Q., Li, C., Xue, Z., Luo, J., 2020a. Continuous waste activated sludge and food waste co-fermentation for synchronously recovering vivianite and volatile fatty acids at different sludge retention times: performance and microbial response. Bioresour. Technol. 313, 123610 https://doi.org/10.1016/j.biortech.2020.123610.

Wu, Y., Luo, J., Zhang, Q., Aleem, M., Fang, F., Xue, Z., Cao, J., 2019. Potentials and challenges of phosphorus recovery as vivianite from wastewater: a review. Chemosphere 226, 246–258. https://doi.org/10.1016/j.chemosphere.2019.03.138.

Yee, M.O., Rotaru, A.E., 2020. Extracellular electron uptake in Methanosarcinales is independent of multiheme c-type cytochromes. Sci Rep. 10 (1) https://doi.org/10.1038/s41598-019-57206-z.

Zachara, J.M., Kukkadapu, R.K., Fredrickson, J.K., Gorby, Y.A., Smith, S.C., 2002. Biomineralization of poorly crystalline Fe(III) oxides by dissimilatory metal reducing bacteria (DMRB). In Geomicrobiol. J. 19 (2) https://doi.org/10.1080/01490450252864271. VolIssue.

Zhang, C., Hu, D., Yang, R., Liu, Z., 2020. Effect of sodium alginate on phosphorus recovery by vivianite precipitation. J. Environ. Sci. (China) 93, 164–169. https://doi.org/10.1016/j.jes.2020.04.007.

Zhuang, K., Izallalen, M., Mouser, P., Richter, H., Risso, C., Mahadevan, R., Lovley, D.R., 2011. Genome-scale dynamic modeling of the competition between Rhodoferax and Geobacter in anoxic subsurface environments. ISME J. 5 (2), 305–316. https://doi.org/10.1038/ismej.2010.117.